# A SINGLE-APERTURE DUPLEX ANTENNA WITH DUAL CIRCULAR POLARIZATIONS

**Yun-Long Lu[1], Yi Wang[2], Steven Gao[3], Changzhou Hua[1], and Taijun Liu[1]**
[1]Faculty of Electrical Engineering and Computer Science, Ningbo University, Ningbo, Zhejiang, 315211, China; Corresponding author: luyunlong@nbu.edu.cn.
[2]Department of Engineering Science, University of Greenwich, ME4 4TB, Kent, United Kingdom
[3]School of Engineering and Digital Arts, University of Kent, Canterbury CT2 7NZ, U.K.

**ABSTRACT***: This letter proposes a novel design of a compact single-aperture dual circular polarization (CP) antenna with integrated duplexing functions using a phase controllable coupled resonator structure. To the best of the authors' knowledge, this is the first report of a multifunctional CP antenna with integrated duplexing performance and dual polarizations. The two orthogonal CPs are realized for the two respective filtering channels. Each channel contains a phased filtering power divider forming the dual-feed to a patch to achieve right-hand or left-hand circular polarization (RHCP or LHCP). The required output phases of the dividers are realized by varied configurations of the coupled λ/2-resonator pairs. A duplex-CP-antenna with RHCP/ LHCP at the downlink/uplink (2.45/2.7 GHz) is designed, fabricated and measured. It achieved a 3-dB AR bandwidth of 3.2%/7.7% at the downlink/uplink and an isolation better than 20 dB. Meanwhile, the antenna showed expected 2nd-order filtering characteristics at both channels.*

**Key Words:** Filtering antenna, duplexer, circular polarization

## 1. INTRODUCTION

In a frequency division duplexing system, antenna and duplexer are the indispensable components in the RF front-end circuits [1]. Duplexers are often employed to separate the uplink and downlink channels operating at different frequencies but share a common antenna [2]. Commonly, a duplexer is composed of two channel filters, suitably combined together with high isolation and good frequency selectivity [3, 4]. It then connects with the antenna at its common port as illustrated in Figure 1(a).

To reduce the volume and complexity of RF front-ends, incorporating antennas and duplexers into a single component without the need of the 50 Ω interfaces between them is considered a favorable solution [5, 6], as illustrated in Figure 1(b). Various integration schemes have been reported [7-9]. In [7], a filtering diplexing antenna with two widely separated operation bands was presented. Another highly integrated duplex antenna with closely located frequency bands was achieved in [8, 9]. However, up to now all the reported duplexer-antennas are linearly polarized. For applications in satellite communications, radio frequency identifications (RFID) and wireless power transmissions, circular polarization (CP) antennas are more desirable for their capabilities of reducing polarization mismatch and suppressing multipath interferences. Therefore, it is very useful to investigate the design of duplex antennas with CP as well as with different polarizations at the downlink and uplink channels. Figure 1(c) illustrates such a system to be demonstrated in this work.

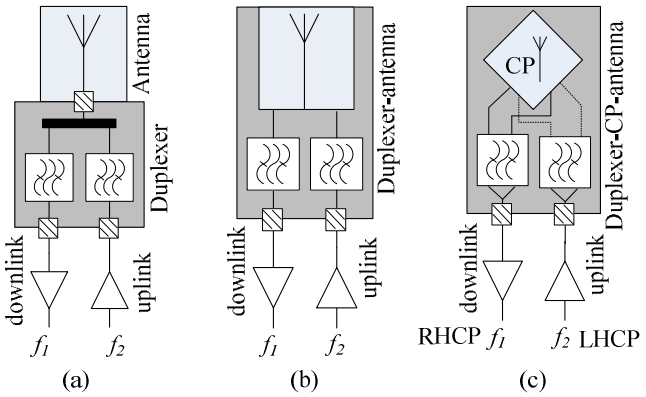


**Figure 1** Block diagrams of (a) a traditional cascaded subsystem, (b) an integrated duplex-antenna subsystem and (c) the integrated duplex-CP-antenna subsystem proposed in this work.

In this letter, a phase-controllable coupled resonator structure is applied for the first time to CP antenna designs to realize the circular polarizations and to provide embedded duplexing functions. The proposed CP antenna uses a dual-feed structure for each channel, with the two channels sharing a single aperture. The feeding structure for each channel is a three-port network, essentially a filtering power divider with controllable output phase, enabled by a coupled-resonator-pair structure. Phase difference of +90° or -90° can be realized to generate the right-hand or left-hand circular polarizations (RHCP and LHCP) at the down- and up-link channels. For demonstration, a duplex antenna with RHCP/ LHCP at the downlink/uplink frequencies of 2.45/2.7 GHz is designed, fabricated and measured.

## 2. DESIGN AND ANALYSIS

### *2.1. Feeding structure to the CP antenna*

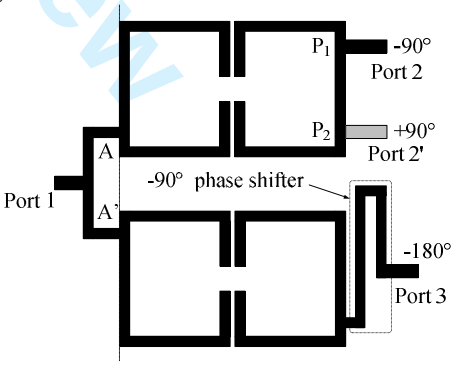


**Figure 2** Feeding structure of the CP antennas – a phased power divider with embedded filtering functions and phase control.

The CP antennas in this paper adopt a novel dual-feed structure that uses coupled λ/2-resonator pairs to provide the required phases and filtering function. It is essentially a phased power divider with a 2nd order filtering characteristic as shown in Figure 2. The amplitude and phase characteristics of the resonator pair have been investigated in [10] and [11]. It

has been shown that its output phase can be switched between +90° and -90°, depending on the tap position of the output port. If the I/O ports are diagonal as in the case of feeding points A and $P_1$ (Figure 2), the phase is -90°. If they are on the same side as in the case of A and $P_2$, the phase is +90°. For the first time, this property has been utilized to feed CP antennas and to control their polarizations in this work.

In Figure 2, the input signal from Port 1 is divided in two ways to Port 2 and 3. The branch to Port 3 contains one coupled resonator pair with a diagonal I/O configuration and one fixed -90° phase shifter. Taking the A-A' plane as the phase reference, it gives Port 3 an output phase of -180°. If Port 2 is tapped to $P_1$, the output phases at Port 2 and 3 become -90° and -180° (Case I). When Port 2 moves to $P_2$, the phases at Port 2' and 3 are changed to +90° and -180° (Case II). Therefore, by adjusting the tap position of Port 2, the phase differences between Port 2 and 3 can be switched between +90° (Case I) and -90° (Case II). By using these two different configurations in the duplex- antenna, the two orthogonal CPs can be realized.

*2.2. Duplex-CP-Antenna*

Now we apply the feeding structure in Figure 2 to a duplex-CP-antenna, as illustrated in Figure 1(c), with the downlink ($f_1$) and uplink ($f_2$) frequencies of 2.45 GHz and 2.7 GHz. The two duplexing channel filters are implemented using two phased filtering power dividers, feeding to a single square patch at different positions as shown in Figure 3. The antenna consists of two substrates (Substrate #1 and #2) of the same sizes and separated by $h$. The radiation patch lies on the top side of Substrate #1, and the two phased power dividers and its ground plane are printed on the top and bottom sides of Substrate #2. The patch is fed by the two power dividers via four metal probes. The length $L_a$ of the patch is approximately a half of the guided wavelength at $f_1$. All the substrates used in this work are Rogers 4350B, with a relative permittivity $\varepsilon_r$ of 3.48, the thickness $h_1$ of 0.762 mm and loss tangent of 0.002. All simulations are carried out using HFSS.

**TABLE 1 Parameters of proposed duplex-CP-antenna (mm)**

| | | | | |
|---|---|---|---|---|
| $L_s$=100 | $h$=10 | $h_1$=0.762 | $L_a$=45 | $d_1$=9.1 |
| $d_2$=22.1 | $d_3$=11.7 | $d_4$=19.5 | $d_5$=1.14 | $d_6$=1 |
| $D_1$=1.28 | $D_2$=2.2 | $L_1$=9.45 | $L_2$=9.45 | $L_3$=3.225 |
| $L_4$=8.6 | $L_5$=8.6 | $L_6$=2.8 | $W_1$=1.68 | $W_2$=0.93 |
| $W_3$=0.8 | $W_4$=0.6 | $W_5$=0.5 | | |

The probe positions, $N_1$ and $N_2$ for the lower band and $N_3$ and $N_4$ for the upper band in Figure 3(c), are optimized to realize the impedance matching. The geometry parameters of the proposed duplex antenna are listed in Table 1. When the patch is fed at $N_1$ and $N_2$, the two points have a phase difference of +90°, so the RHCP is excited at the lower band. To achieve the LHCP at the upper band, the phase properties at $N_3$ and $N_4$ can either be Case I (-90°, -180°) or Case II (-180°, +90°), the corresponding feeding structures of which are given in Figure 3(d). Figure 4 compares the LHCP performances of both cases. It was found that their impedance bandwidths and gain responses are similar, but the axial ratio (AR) bandwidth of Case II is wider than Case I. Therefore the Case II design is chosen for the upper band.

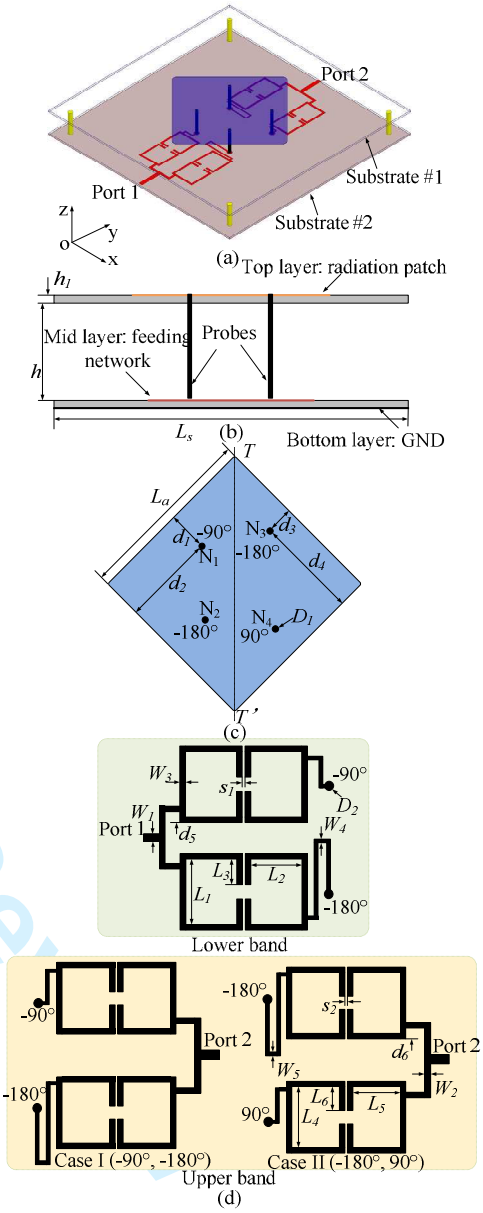


**Figure 3** Duplex-CP-antenna configuration. (a) 3D view; (b) Side view; (c) Radiation patch; (d) Feeding networks for the lower and upper band.

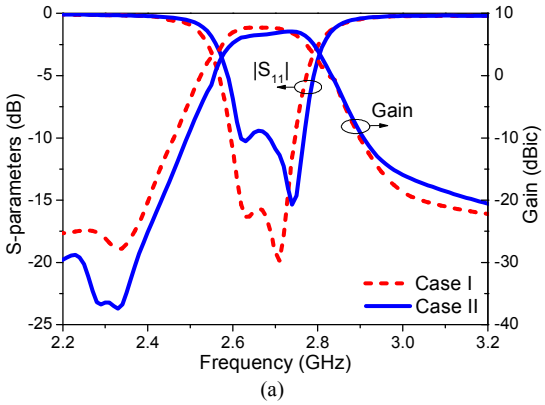

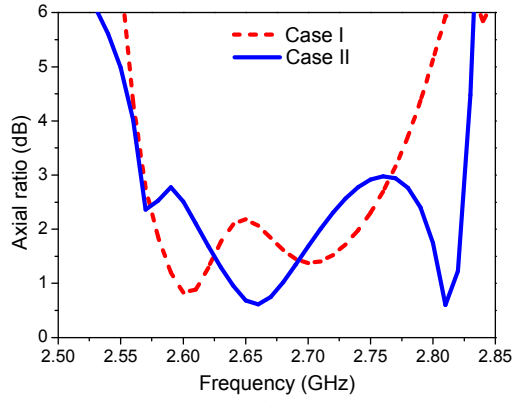


(b)

**Figure 4** Comparison of the simulated (a) $|S_{11}|$, gains and (b) AR at the upper band between Case I ($N_3$: -90°, $N_4$: -180°) and Case II ($N_3$: -180°, $N_4$: +90°).

## 3. RESULTS AND DISCUSSION

In order to demonstrate the design concept, a porotype was fabricated and tested. All the reflection coefficients are measured using an Agilent 8361C network analyzer. The radiation patterns, axial ratios and antenna gains are measured using a SATIMO SG24 near-field measurement system.

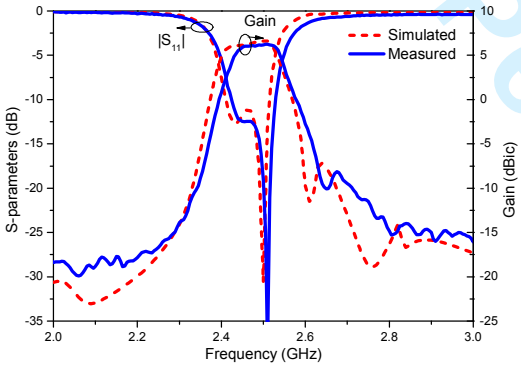


(a)

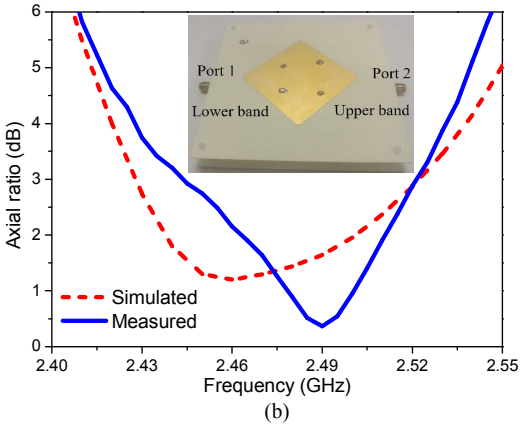


(b)

**Figure 5** Measured and simulated (a) reflection coefficients, gains and (b) AR when Port 1 is excited and Port 2 is terminated with a 50 Ω load for the RHCP at the lower band. The inset shows the fabricated prototype.

The measured reflection coefficients and gains of the RHCP are shown in Figure 5(a), when Port 1 is excited. They are in reasonably good agreement with simulations. The impedance bandwidth ($|S_{11}|$ < -10 dB) is 4.1% (2.42-2.52 GHz), and the measured gain curve is desirably flat across the passbands with an average in-band gain of 5.8 dBic and maximum gain of 6.2 dBic. At 100 MHz outside the passband, the measured rejection is over 12.9 dB at 2.32 GHz and 9.3 dB at 2.63 GHz. The gain is suppressed to below -9.2 dBic at the center frequency of the upper band (2.69 GHz). Figure 5(b) shows the measured and simulated AR of the RHCP. The measured AR bandwidth is 3.2% from 2.44 to 2.52 GHz.

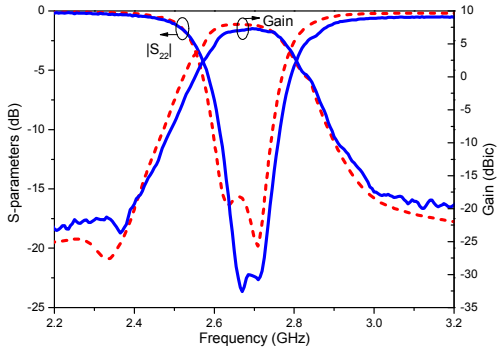


(a)

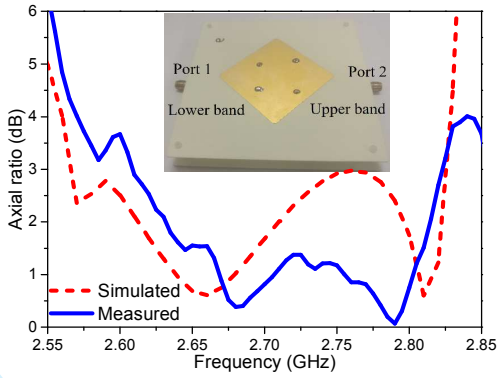


(b)

**Figure 6** Measured and simulated (a) reflection coefficients, gains and (b) AR when Port 1 is terminated with a 50 Ω load and Port 2 is excited for the LHCP at the upper band.

The measured reflections and gains of the LHCP at the upper band are shown in Figure 6(a). The impedance bandwidth ($|S_{22}|$ < -10 dB) is 5.2% (2.62-2.76 GHz) with an average in-band gain of 6.8 dBic and maximum gain of 7.2 dBic. At 100 MHz outside the passband, the measured rejection is over 9.9 dB at 2.52 GHz and 10.3 dB at 2.86 GHz. The gain is suppressed to below -13.7 dBic at the center frequency of the lower band (2.47 GHz). From Figure 6(b), the measured AR bandwidth is 7.7% from 2.61 to 2.82 GHz.

When Port 1 is excited and Port 2 is terminated with a 50 Ω load, the measured and simulated normalized radiation patterns at the lower band are shown in Figure 7(a). The measured co-polarization in the boresight is at least 24 dB higher than the cross-polarization, and the measured front-to-back ratio is over 16 dB across the operation band. The 3-dB beam-widths in the φ=0° and 90° patterns are 65° and 67°. For the upper band when Port 1 is terminated with a 50 Ω load and Port 2 is excited, the measured and simulated radiation patterns are shown in Figure 7(b). The measured co-polarization in the boresight is at least 23 dB higher than the cross-polarization, and the measured front-to-back ratio is over 12 dB across the operation band. The 3-dB beam-widths in the φ=0° and 90° patterns are 57° and 63°.

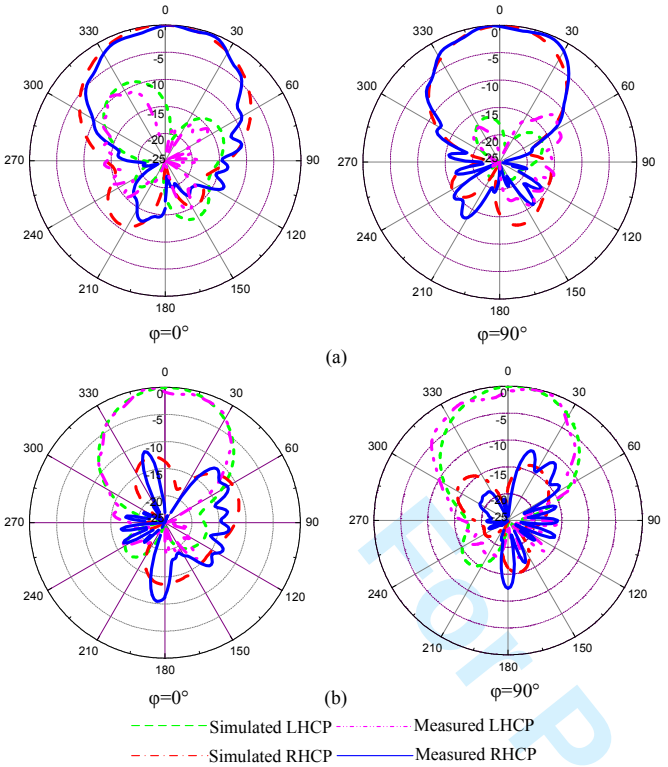


**Figure 7** Normalized radiation patterns at (a) 2.47 GHz when Port 1 was excited and (b) 2.69 GHz when Port 2 was excited.

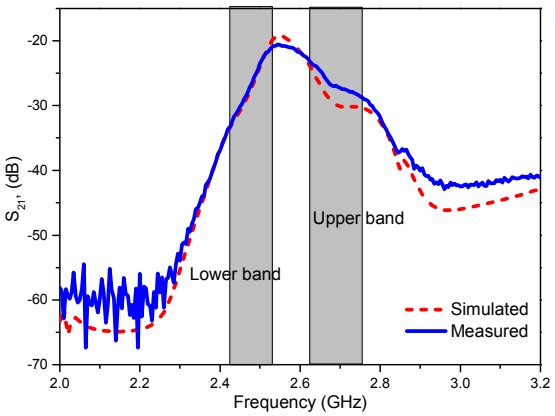


**Figure 8** Simulated and measured isolation of the duplex antenna with the shaded areas indicating the two operation bands.

**TABLE 2 Performance comparison of integrated duplex-antennas**

| | [7] | [8] | [9] | This work |
|---|---|---|---|---|
| Frequency (GHz) | 2.45/5.25 | 1.97/2.08 | 2.57/2.88 | 2.45/2.7 |
| Isolation (dB) | >21 | >14 | >32 | >20 |
| Peak gain (dBi) | 2.3/2.6 | 5/5 | 5/4.5 | 6.2/7.2** |
| Cross-Pol. (dB) | >18 | - | >20 | >23 |
| Polarization | Linear | Linear | Linear | RH/LHCP |
| Gain supp.* (dB) | >7.8 | - | >15 | >9.3 |

* 100 MHz away from the edges of passband.
** The unit of peak gain in this work is dBic.

The inter-channel isolation $S_{21}$ of the duplex CP antenna is shown in Figure 8. The measured results agree very well with the simulation, showing an isolation of over 20.3 dB in the downlink channel (2.42 to 2.52 GHz) and over 22.7 dB in the uplink (2.62 to 2.76 GHz). Table 2 compares the performance of the proposed duplex-CP-antenna with other published integrated duplex-antennas. The proposed antenna, uniquely having dual CPs, also exhibits very competitive isolation, in-band gain and out-of-band rejection. It has the highest cross-polarization level of 23 dB.

## 4. CONCLUSION

The single-aperture duplex antenna with orthogonal circular polarizations is proposed and analyzed in this paper. A three-port feeding structure, which functions as a filtering power divider with controllable output phase, has been applied to generate the LHCP and RHCP. A duplex-antenna at 2.45 GHz (downlink) and 2.7 GHz (uplink) was demonstrated to have an inter-channel isolation of over 20 dB. This is the first integrated duplexer-antenna with dual circular polarizations. The compact structure and integrated function can be explored in satellite and mobile communication systems for reducing polarization mismatch, alleviating multipath or polarization diversity.

## 5. ACKNOWLEDGMENT

This work was supported in part by NSFC 61571251 and 61631012, partly by Zhejiang Natural Science Foundation LQ17F010002 and K.C. Wong Magna Fund in Ningbo University. The work of Yi Wang was supported by UK EPSRC under Contract EP/M013529/1.

## REFERENCES

[1] X. Y. Zhang, Y. Zhang, Y.-M. Pan, and W. Duan, Low-profile dual-band filtering patch antenna and its application to LTE MIMO system, IEEE Trans Antennas Propag 65 (2017), 103–113.
[2] X. Shang, Y. Wang, W. Xia, M. J. Lancaster, Novel Multiplexer Topologies Based on All-Resonator Structures, IEEE Trans Microwave Theory Tech 61 (2013) , 3838-3845.
[3] M. Li, K.-D. Xu, J. Ai, and Y. Liu, Compact diplexer using short stub-loaded composite right/left-handed resonator, Microwave Opt Technol Lett 59 (2017), 1470–1474.
[4] T. Yang, and G. M. Rebeiz, A simple and effective method for 1.9–3.4-GHz tunable diplexer with compact size and constant fractional bandwidth, IEEE Trans Microwave Theory Tech 64 (2016), 436–449.
[5] C.-X. Mao, S. Gao, Y. Wang, Q. Luo, and Q.-X. Chu, A shared-aperture dual-band dual-polarized filtering-antenna-array with improved frequency response, IEEE Trans Antennas Propag 65 (2017), 1836-1844.
[6] C.-Y. Hsieh, C.-H. Wu, and T.-G. Ma, A compact dual-band filtering patch antenna using step impedance resonators, IEEE Antennas Wireless Propag Lett 14 (2015), 1056–1059.
[7] Y.-J. Lee, J.-H. Tarng, and S.-J. Chung, A filtering diplexing antenna for dual-band operation with similar radiation patterns and low cross-polarization levels, IEEE Antennas Wireless Propag Lett 16 (2017), 58-61.
[8] H. M. Hizan, I. C. Hunter, and A. I. Abunjaileh, Integrated dual-band radiating bandpass filter using dual-mode circular cavities, IEEE Microwave Wireless Compon Lett 21 (2011), 246–248.
[9] C.-X. Mao, S. Gao, Y. Wang, F. Qin, and Q.-X. Chu, Compact highly integrated planar duplex antenna for wireless communications, IEEE Trans Microwave Theory Tech 64 (2016), 2006–2013.
[10] Y.-L. Lu, Y. Wang, C. Hua, and T. Liu, Design of compact filtering rat-race hybrid with λ/2-resonators, Electron Lett 52 (2016), 1780-1782.
[11] Y. C. Li, Q. Xue, and X. Y. Zhang, Single- and dual-band power dividers integrated with bandpass filters, IEEE Trans Microwave Theory Tech 61 (2013), 69–76.

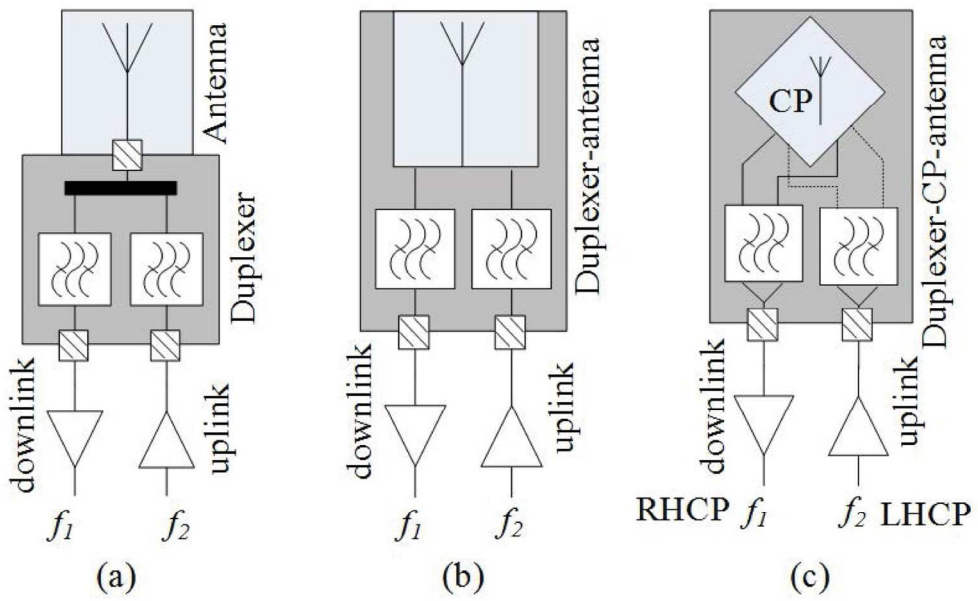


Figure 1 Block diagrams of (a) a traditional cascaded subsystem, (b) an integrated duplex-antenna subsystem and (c) the integrated duplex-CP- antenna subsystem proposed in this work.

130x79mm (300 x 300 DPI)

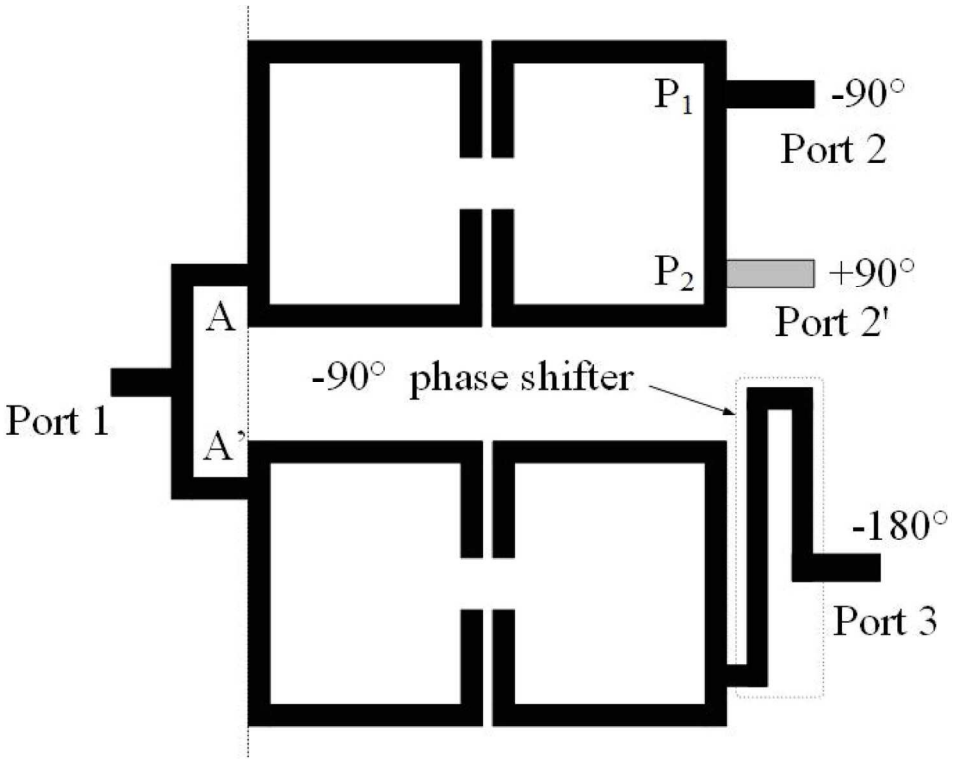


Figure 2 Feeding structure of the CP antennas – a phased power divider with embedded filtering functions and phase control.

143x108mm (300 x 300 DPI)

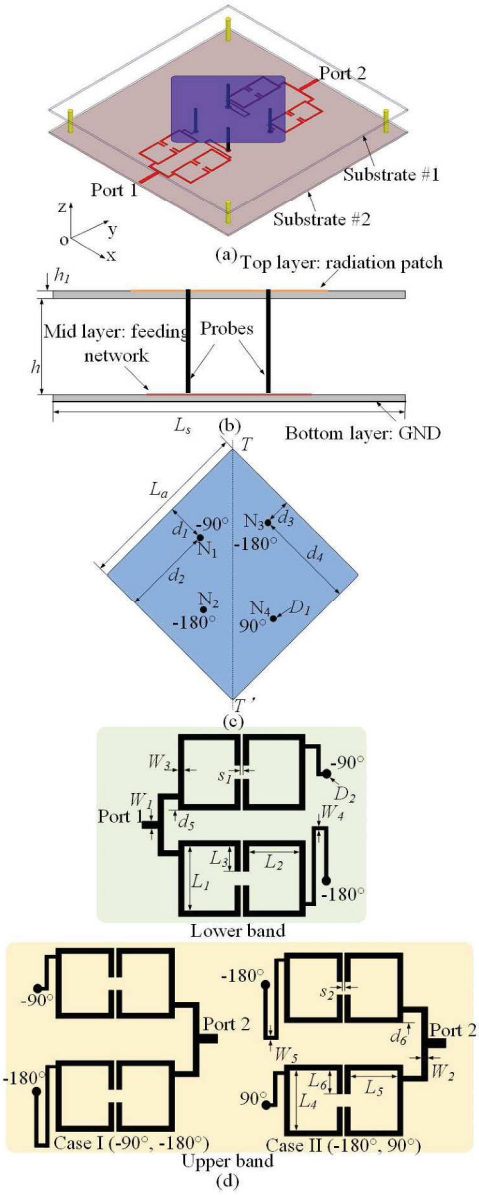


Figure 3 Duplex-CP-antenna configuration. (a) 3D view; (b) Side view; (c) Radiation patch; (d) Feeding networks for the lower and upper band.

517x1256mm (300 x 300 DPI)

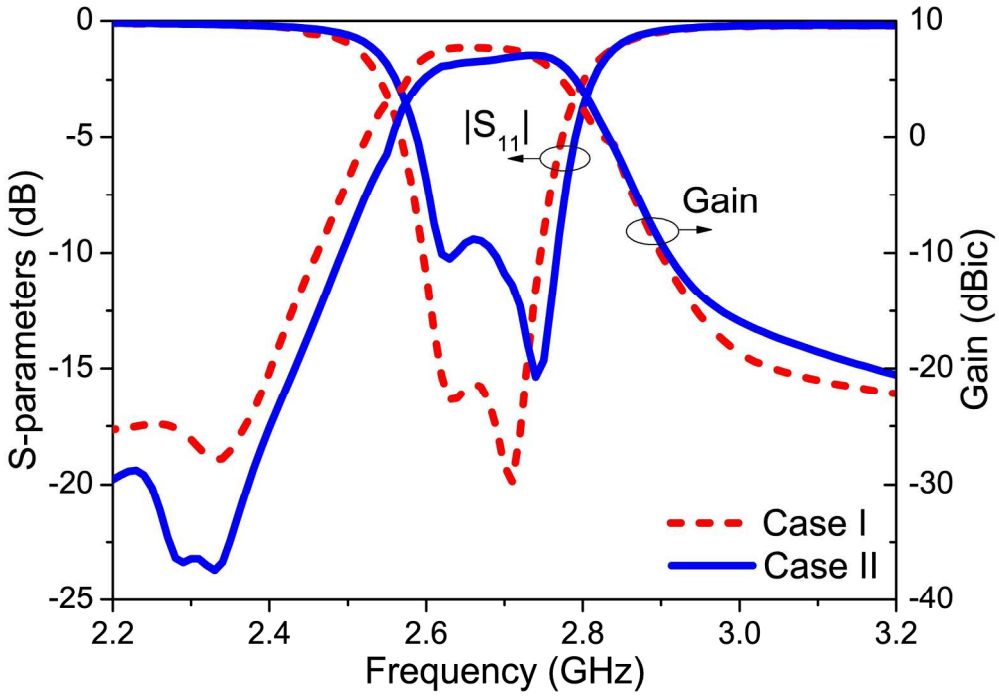


Figure 4 Comparison of the simulated (a) |S11|, gains and (b) AR at the upper band between Case I (N3: -90°, N4: -180°) and Case II (N3: -180°, N4: +90°).

199x139mm (300 x 300 DPI)

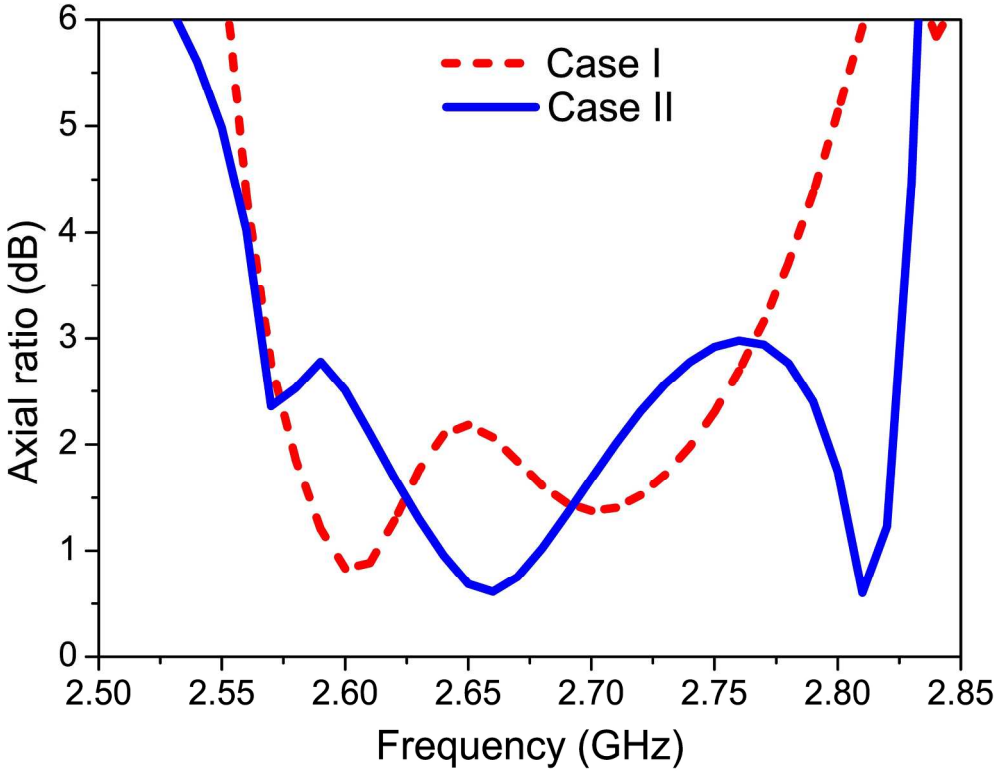


Figure 4 Comparison of the simulated (a) |S11|, gains and (b) AR at the upper band between Case I (N3: -90°, N4: -180°) and Case II (N3: -180°, N4: +90°).

222x172mm (300 x 300 DPI)

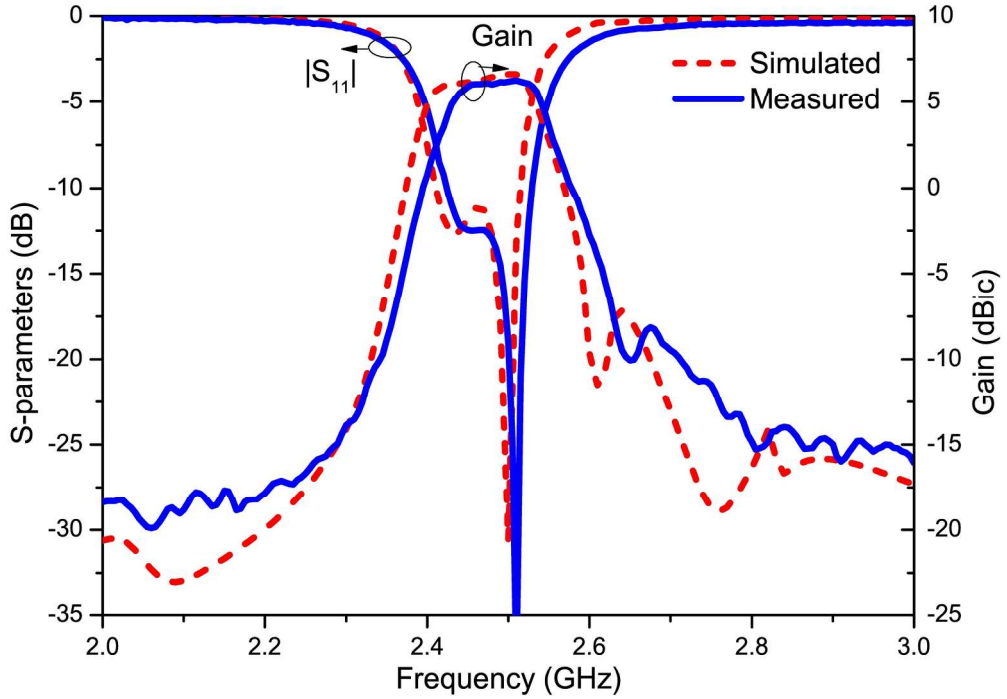


Figure 5 Measured and simulated (a) reflection coefficients, gains and (b) AR when Port 1 is excited and Port 2 is terminated with a 50 Ω load for the RHCP at the lower band. The inset shows the fabricated prototype.

200x140mm (300 x 300 DPI)

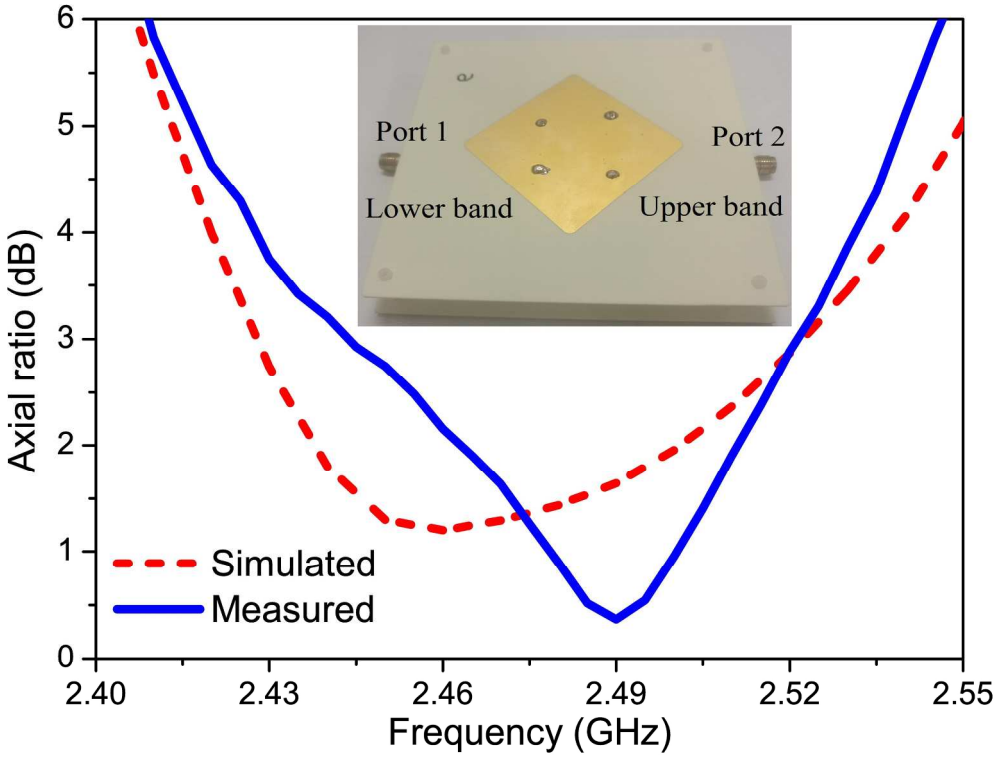


Figure 5 Measured and simulated (a) reflection coefficients, gains and (b) AR when Port 1 is excited and Port 2 is terminated with a 50 Ω load for the RHCP at the lower band. The inset shows the fabricated prototype.

218x166mm (300 x 300 DPI)

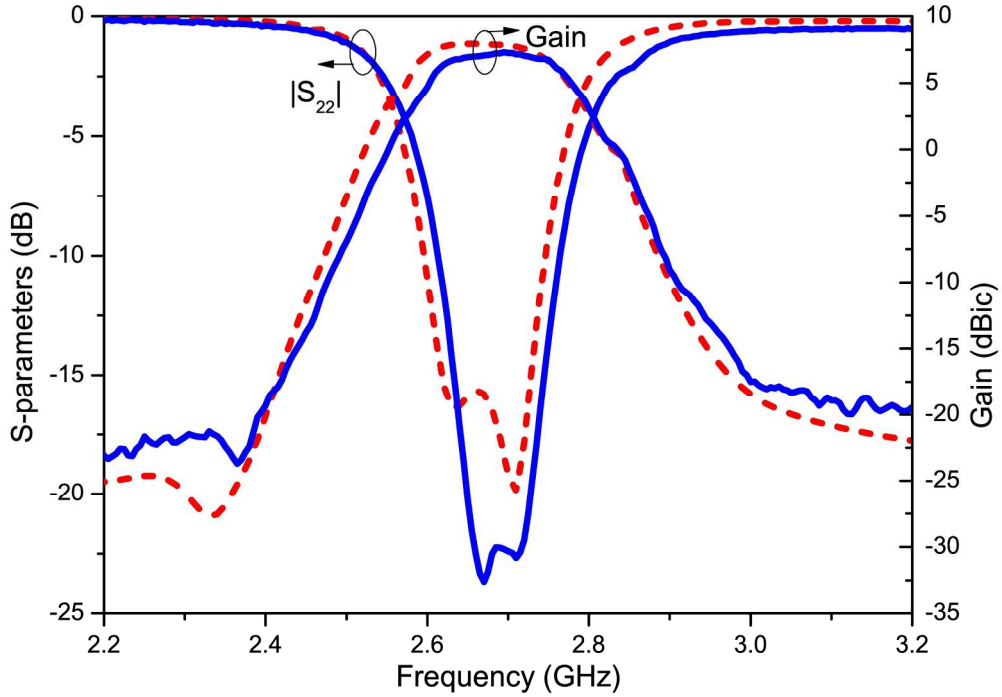


Figure 6 Measured and simulated (a) reflection coefficients, gains and (b) AR when Port 1 is terminated with a 50 Ω load and Port 2 is excited for the LHCP at the upper band.

200x139mm (300 x 300 DPI)

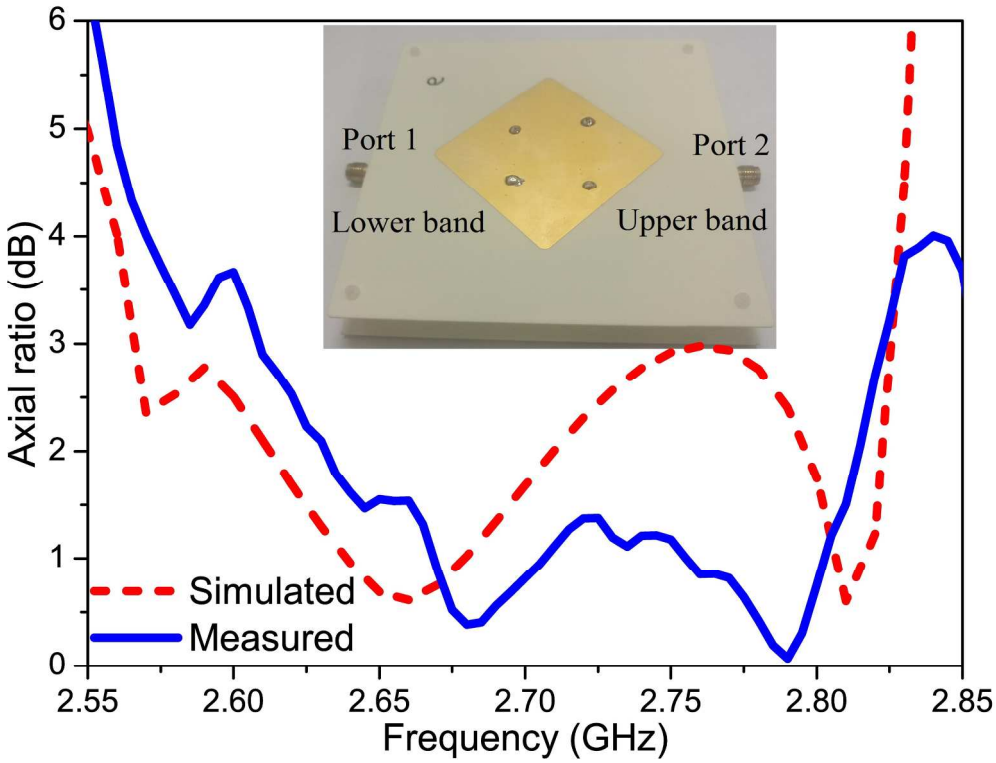


Figure 6 Measured and simulated (a) reflection coefficients, gains and (b) AR when Port 1 is terminated with a 50 Ω load and Port 2 is excited for the LHCP at the upper band.

219x167mm (300 x 300 DPI)

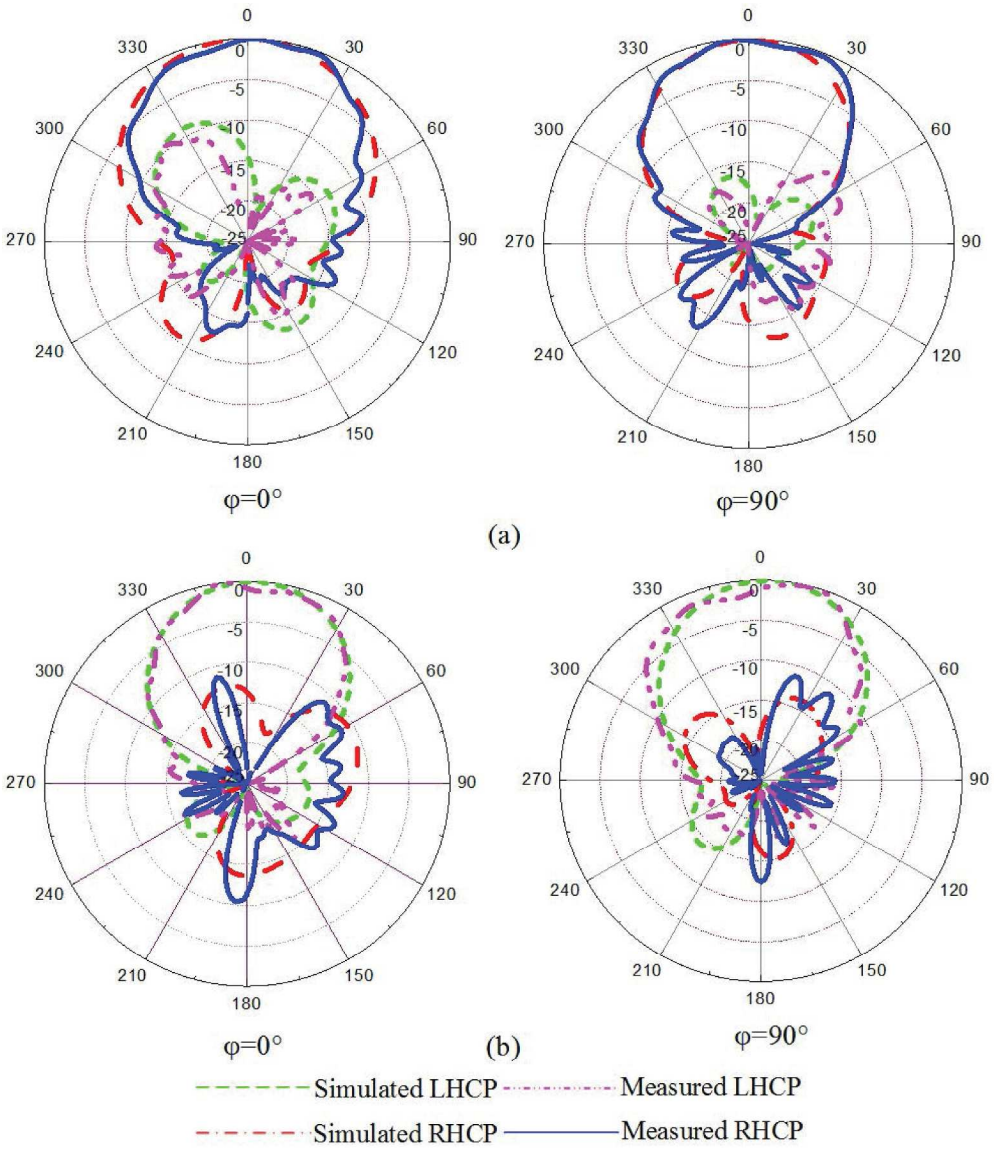


Figure 7 Normalized radiation patterns at (a) 2.47 GHz when Port 1 was excited and (b) 2.69 GHz when Port 2 was excited.

305x353mm (300 x 300 DPI)

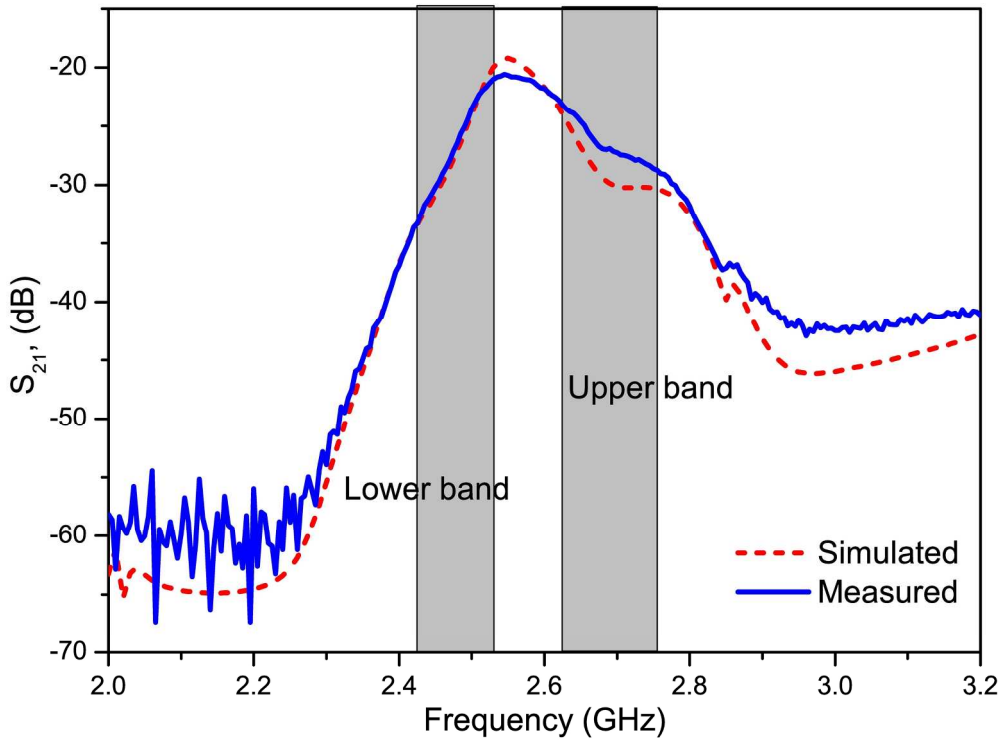


Figure 8 Simulated and measured isolation of the duplex antenna with the shaded areas indicating the two operation bands.

210x155mm (300 x 300 DPI)